# Full Articles

## Primary photophysical and photochemical processes upon UV excitation of $PtBr_6^{2-}$ and $PtCl_6^{2-}$ complexes in water and methanol*

*I. P. Pozdnyakov,[a,b] E. M. Glebov,[a,b]* S. G. Matveeva,[a] V. F. Plyusnin,[a,b] A. A. Mel´nikov,[c] and S. V. Chekalin[c]*

[a]*Voevodsky Institute of Chemical Kinetics and Combustion, Siberian Branch of the Russian Academy of Sciences, 3 ul. Institutskaya, 630090 Novosibirsk, Russian Federation. Fax: +7 (383) 330 7350. E-mail: glebov@kinetics.nsc.ru*
[b]*Novosibirsk National Research State University, 2 ul. Pirogova, 630090 Novosibirsk, Russian Federation*
[c]*Institute for Spectroscopy, Russian Academy of Sciences, 5 ul. Phisicheskaya, 142190 Moscow, Russian Federation*

Primary photophysical and photochemical processes were studied for $Pt^{IV}Br_6^{2-}$ and $Pt^{IV}Cl_6^{2-}$ complexes in water and methanol by ultrafast kinetic spectroscopy upon excitation in the band region of charge transfer from the ligand-centered group π-orbitals to the $e_g$*-orbital of $Pt^{IV}$ complex anion (LMCT bands). The data obtained earlier upon excitation in the region of d—d bands were compared. Irrespective of the excitation wavelength, the photochemical properties of complexes are caused by the reactions of intermediates proceeding in the picosecond time range. These intermediates were identified as $Pt^{IV}Br_5^-$ upon photolysis of $Pt^{IV}Br_6^{2-}$ and, presumably, the Adamson radical pair $[Pt^{III}Cl_5^{2-}(C_{4v})...Cl^{\bullet}]$ upon photolysis of $Pt^{IV}Cl_6^{2-}$. The difference in the exciting light wavelengths has an impact only on the first step of these processes, *i.e.*, transition from the Franck—Condon excited state to intermediates.

**Key words:** photochemistry, platinum(IV) halide complexes, aqueous and alcoholic solutions, ultrafast kinetic spectroscopy, primary photophysical and photochemical processes.

The photochemical activity of platinum compounds was reported first in 1832.[1] In that work, the research object was $Pt^{IV}Cl_6^{2-}$ complex in modern terminology. Over 150 years, the photochemistry of $Pt^{IV}$ halide complexes was of pure academic interest,[2—5] which was due to a variety of photoprocesses, especially for hexachloroplatinate. The interest arose from three aspects: 1) a great number of intermediates mainly identified as $Pt^{III}$ complexes,[6—12] 2) unusual chain photochemical aquation,[10,11] and 3) hard-to-explain differences in the photochemical prop-

* Based on the materials of the XXVI International Chugaev Conference on Coordination Chemistry (October 6—10, 2014, Kazan).

Published in Russian in *Izvestiya Akademii Nauk. Seriya Khimicheskaya,* No. 8, pp. 1784—1795, August, 2015.
1066-5285/15/6408-1784 

erties of $Pt^{IV}Cl_6^{2-}$ and $Pt^{IV}Br_6^{2-}$ complexes having similar structures of valence-shell orbitals.[2,3]

In 1980s, the photochemistry of platinum-metal halide complexes got an impetus to development caused by practical tasks. The discovered[13,14] four-electron photoreduction of $Pt^{IV}$ to $Pt^0$ in water—methanol mixtures has been being used extensively for the preparation of platinum nanoparticles.[15—22] In photocatalysis, the surface modification (typically, photochemical) of $TiO_2$ (see Refs 23—26) and CdS (see Refs 27 and 28) with platinum-metals complexes shifts the absorption spectrum of semiconductors to the visible spectral region. Finally, the photodynamic therapy (PDT) of malignancies is a rapidly developing application field of platinum complexes. The use of platinum complexes in PDT (see Refs 29—31) brings a hope for the design of medical technique combining the cytotoxcity of platinum complexes and particular advantages of PDT (selectivity and lower toxicity).

A successful application of photochemistry in photocatalysis and PDT requires detailed data on the reaction mechanisms. To build the fully proved mechanism of photochemical reaction, one should trace the whole transformation pathway from primary physical processes to the formation of final products. Historically, the mechanisms of photolysis of coordination compounds were proposed based on the data from steady-state studies.[2—5] In some cases, the formation of unobserved short-lilving reactive intermediate species, such as Adamson radical pairs, was postulated.[32] At the present time, intermediates can be detected directly in femtosecond time-resolved experiments. In particular, the primary photophysical and photochemical processes have been studied for the platinum-metal complexes: $Pt^{IV}Br_6^{2-}$,[10,33—36] $Pt^{IV}Cl_6^{2-}$,[10,36] $Ir^{IV}Cl_6^{2-}$,[37—39] $Ir^{IV}Br_6^{2-}$,[35,40] and $Os^{IV}Br_6^{2-}$.[35]

In the works on ultrafast kinetic spectroscopy of $Pt^{IV}Br_6^{2-}$ (see Refs 10, 33, and 36) and $Pt^{IV}Cl_6^{2-}$ complexes[10,36] in aqueous and alcoholic solutions, the laser excitation in the range from 400 to 420 nm was used. These complexes are known to show different photochemical behavior in aqueous solutions upon change in the wavelength. The quantum yield of $Pt^{IV}Br_6^{2-}$ photoaquation does not depend on the radiation wavelength.[41,42] However, such dependence was observed for the $Pt^{IV}Cl_6^{2-}$ complex.[12] The present work describes experiments on femtosecond kinetic spectroscopy of the $PtBr_6^{2-}$ and $Pt^{IV}Cl_6^{2-}$ complexes in water and methanol upon near-UV excitation (320 nm). The aim was to compare the processes initiated by excitation of complexes into different electronic states.

## Experimental

Experiments on ultrafast kinetic spectroscopy were performed on the earlier described device.[43] Excitation was performed using pulses with a time of ~100 fs at 320 nm (fourth harmonic of the signal wave of TOPAS parametric amplifier). A portion of exciting laser beam was focused on a cell with water to generate a probe radiation (continuum). The pulse energy was ~1 μJ at the repetition frequency of 1 kHz. 200 laser pulses were used to record one spectrum of intermediate absorption with certain time delay between the exciting and probing pulses. The optical path length of a cell was 1 mm; a flow system with a total volume of 10 mL was used to provide the homogeneity of irradiation and to decrease the photodegradation effect. Experimental data were approximated by the global fit of kinetic curves with one set of parameters. We performed the chirp correction of group velocity dispersion and calculated the response function using a processing program.

Electronic absorption spectra were recorded on an Agilent 8453 spectrophotometer (Agilent Technologies). The steady-state photolysis was performed using a high-pressure mercury lamp with a set of glass filters for isolation of necessary wavelength or light emitting diodes with a half-height linewidth of ~5 nm. Quantum yields were measured using a 1 cm cell. A solution in the cell was stirred with a magnetic stirrer. The light source intensity required for calculation of quantum yields was measured with a SOLO 2 power meter (Gentec EO).

Solutions of the $Pt^{IV}Br_6^{2-}$ complex were prepared from $Na_2PtBr_6 \cdot H_2O$ synthesized according to the earlier described procedure.[44] The $Pt^{IV}Cl_6^{2-}$ ion source was $Na_2PtCl_6$ (Aldrich) and solutions were prepared using deionized water and spectroscopy-grade methanol (Aldrich). The purity of solvents was controlled by spectrophotometry.

## Results and Discussion

**Electronic absorption spectra and photochemistry of $Pt^{IV}Br_6^{2-}$ and $Pt^{IV}Cl_6^{2-}$ complexes.** The electronic absorption spectra (EAS) of complexes in aqueous solutions are shown in Fig. 1. The vertical lines in the figures (including the insert) indicate the wavelengths at which femtosecond experiments were performed in the present and earlier works.[10,33,36] The data on the nature of this absorption bands and photochemical processes in aqueous and alcoholic solutions caused by excitation in the corresponding spectral ranges are summarized in Table 1.

$Pt^{IV}Br_6^{2-}$ and $Pt^{IV}Cl_6^{2-}$ are low-spin octahedral complexes with a $5d^6$ electron configuration. The most intense charge transfer band in the spectrum of $Pt^{IV}Br_6^{2-}$ complex (see Fig. 1) has a maximum at 226 nm. It corresponds to the electron density transfer from the ligand-centered group σ-orbitals to unoccupied σ*-orbitals localized predominantly on the central ion.[45] The less intense charge transfer bands in the range of 290—450 nm correspond to transitions from the ligand-centered group π-orbitals to the group $e_g$*-orbitals of complex anion (LMCT transitions). These LMCT bands partially overlap with d—d bands.[45] The charge transfer band with a maximum at 311 nm corresponds to the transitions $\pi(t_{2u}) \rightarrow d(e_g^*)$ and $\pi(t_{1u}) \rightarrow d(e_g^*)$.[35,45] According to calculations,[34,35] the absorption at 400—420 nm corresponding to excitation of the complex in the femtosecond experiments[10,33,36]

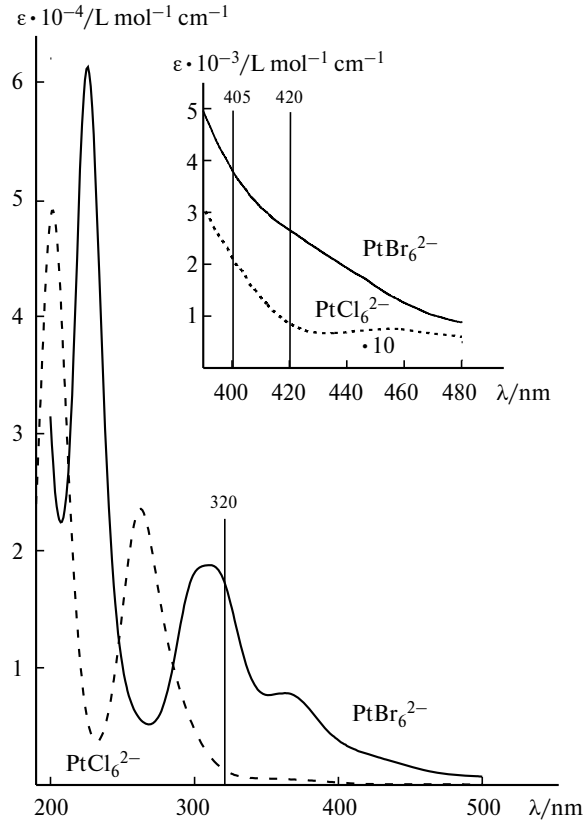


**Fig. 1.** Electronic absorption spectra for the $PtBr_6^{2-}$ and $PtCl_6^{2-}$ complexes in aqueous solutions. The insert shows the visible spectral region (blue region). The vertical lines denote the excitation wavelengths used in the ultrafast kinetic spectroscopy study.

is caused by the LMCT transition $\pi(^1t_{1g}) \rightarrow d(e_g^*)$ (401 nm) and the d—d transition $d(t_{2g}) \rightarrow d(e_g^*)$ (413 nm). Both transitions are forbidden.

The spectrum of the chloride complex compared to the bromide one is shifted to shorter wavelengths (see Fig. 1). The most intense LMCT absorption band of $Pt^{IV}Cl_6^{2-}$ with a maximum at 202 nm corresponds to the absorption band of $Pt^{IV}Br_6^{2-}$ with a maximum at 226 nm[47,50] and the less intense absorption band with a maximum at 263 nm corresponds to that at 311 nm in the spectrum of $Pt^{IV}Br_6^{2-}$. The plateau at ~355 nm and the low-intensity broad band at ~455 nm belong to the d—d transitions.[47,50]

Irradiation of aqueous solutions of the $Pt^{IV}Br_6^{2-}$ complex results first in the transformation[41]

$$Pt^{IV}Br_6^{2-} \xrightarrow[H_2O]{h\nu} Pt^{IV}Br_5(H_2O)^- + Br^-. \qquad (1)$$

The quantum yield of reaction (1) is close to 0.4 and does not depend on the radiation wavelength.[41,42] Long-term irradiation[41,42] results in further aquation of $Pt^{IV}Br_5(H_2O)^-$. During nanosecond laser flash photolysis, only instantaneous change in the absorption corresponding to the difference between the optical absorption spectra of $Pt^{IV}Br_5(H_2O)^-$ and $Pt^{IV}Br_6^{2-}$ was observed.[42]

Irradiation of $Pt^{IV}Br_6^{2-}$ in methanol at ~313 nm results[10] in photosolvation to form $Pt^{IV}Br_5(CH_3OH)^-$ and simultaneous two-electron photoreduction to form $Pt^{II}Br_4^{2-}$. The cumulative data for the processes can be described by Eqs (2)—(4). The quantum yield of photoreaction[46] upon excitation in the wavelength range of 254—436 nm is equal to 0.4 regardless of the complex concentration and the exciting light intensity. The ratio between the quantum yields of photosolvation and photoreduction upon irradiation at 313 nm is close[10] to 1.5 and their values are $\varphi_{solv} = 0.24$ and $\varphi_{red} = 0.16$, respectively. The hydroxymethyl radicals do not react with the $Pt^{IV}$ and $Pt^{II}$ complexes at experimentally measurable rate constants.[10]

**Table 1.** Spectroscopic and photochemical characteristics of $PtBr_6^{2-}$ and $PtCl_6^{2-}$ complexes in water and methanol

| Complex | λ/nm | Absorption band | Transition | Photochemical process | |
|---|---|---|---|---|---|
| | | | | $H_2O$ | MeOH |
| $PtBr_6^{2-}$ | 320 | Maximum at 311 nm | LMCT $\pi(t_{2u}) \rightarrow d(e_g^*)$ and $\pi(t_{1u}) \rightarrow d(e_g^*)$[35,45] | Photoaquation, $\varphi_{aq} = 0.4$ (see Refs 41 and 42) | Photosolvation + photoreduction $\varphi \approx 0.4$,[46] $\varphi_{solv} \approx 1.5\varphi_{red}$ (see Ref. 10) |
| | 405—420 | Long-wave end of the intense band at 365 nm + weak band at 435 nm | LMCT $\pi(^1t_{1g}) \rightarrow d(e_g^*)$ and $d(t_{2g}) \rightarrow d(e_g^*)$[35,45] (forbidden) | | |
| $PtCl_6^{2-}$ | 320 | Long-wave end of the intense band at 263 nm + weak LMCT bands at 325 and 329 nm | LMCT $\pi(t_{1u}) \rightarrow d(e_g^*)$ and $d(t_{2g}) \rightarrow d(e_g^*)$[47] | Photoaquation, $\varphi_{aq}$ depends on the wavelength, exciting light intensity, and $PtCl_6^{2-}$ concentration, chain process[12] | Photosolvation + photoreduction[48,49], $\varphi_{solv} \geq 0.6$ (313 nm), $\varphi_{solv} > \varphi_{red}$ |
| | 405—420 | Long-wave end of the weak band at 353 nm | $d(t_{2g}) \rightarrow d(e_g^*)$[47] | Ditto | $\varphi_{solv} \geq 0.1$ |

$$Pt^{IV}Br_6^{2-} \xrightarrow[CH_3OH]{h\nu} Pt^{IV}Br_5(CH_3OH)^- + Br^- \quad (2)$$

$$Pt^{IV}Br_6^{2-} \xrightarrow[CH_3OH]{h\nu} Pt^{III}Br_5^{2-} + {}^{\bullet}CH_2OH + Br^- + H^+ \quad (3)$$

$$Pt^{III}Br_5^{2-} + CH_3OH \longrightarrow Pt^{II}Br_4^{2-} + {}^{\bullet}CH_2OH + Br^- + H^+ \quad (4)$$

Aqueous solutions of the $Pt^{IV}Cl_6^{2-}$ complex are characterized by redox photochemical reactions. Starting from Ref. 51, the majority of papers on the photochemistry of $Pt^{IV}Cl_6^{2-}$ in water consider that the primary process is homolytic cleavage of the Pt—Cl bond to release the Cl atom into the bulk of solvent (reaction (5)). However, the integral photochemical process is photoaquation to form, at the first step, the $Pt^{IV}Cl_5(H_2O)^-$ complex.[9,12,51–55] If the primary process (5) is realized, photoaquation can proceed by the chain mechanism. The analysis of experimental data[9,12,52–55] and data from quantum chemical calculations[56–58] performed in Refs 10 and 36 allows conclusion of that the chain carrier must be a planar trivalent platinum complex with a $Pt^{III}Cl_{4-n}X_n$ structure ($n = 1$—3; $X = OH^-$, $H_2O$). The possible scheme of chain processes involving $Pt^{III}Cl_3(OH)^-$ as the chain carrier is represented by Eqs (6)—(11).

Chain initiation:

$$Pt^{IV}Cl_6^{2-} \xrightarrow{h\nu} Pt^{III}Cl_5^{2-} + Cl^{\bullet}, \quad (5)$$

$$Pt^{III}Cl_5^{2-} + 2\,H_2O \longrightarrow Pt^{III}Cl_4(OH)(H_2O)^{2-} + Cl^- + H^+, \quad (6)$$

$$Pt^{III}Cl_4(OH)(H_2O)^{2-} \longrightarrow Pt^{III}Cl_3(OH)^- + H_2O + Cl^-. \quad (7)$$

Chain propagation:

$$Pt^{III}Cl_3(OH)^- + Pt^{IV}Cl_6^{2-} + H_2O \longrightarrow Pt^{IV}Cl_5(OH)^{2-} + Pt^{III}Cl_3(H_2O) + Cl^-, \quad (8)$$

$$Pt^{III}Cl_3(H_2O) \longrightarrow Pt^{III}Cl_3(OH)^- + H^+, \quad (9)$$

$$Pt^{IV}Cl_5(OH)^{2-} + H^+ \longrightarrow Pt^{IV}Cl_5(H_2O)^-. \quad (10)$$

Chain termination:

$$2\,Pt^{III}Cl_3(OH)^- + 2\,H_2O \longrightarrow Pt^{IV}Cl_4(OH)(H_2O)^- + Pt^{II}Cl_2(OH)(H_2O)^-. \quad (11)$$

The quantum yield of $Pt^{IV}Cl_6^{2-}$ photoaquation ($\varphi_{aq}$) depends on the concentration of starting complex, radiation wavelength, and exciting light intensity.[12] Depending on the experimental conditions, the quantum yield can be both less[9,52,53] and significantly more than unity.[12,43,52] In addition to the chain mechanism, photoaquation can proceed by the non-chain mechanism[10] analogous to that assumed for the photolysis of bromide complex.

For the alcoholic solutions of the $Pt^{IV}Cl_6^{2-}$ complex as for the bromide one, concurrent reactions proceed: photosolvation to form the $Pt^{IV}Cl_5(CH_3OH)^-$ complex (analogously to reaction (2)) and two-electron photoreduction[46] to form the $Pt^{II}Cl_4^{2-}$ complex. The spectral changes corresponding to the initial step of photolysis are shown in Fig. 2, *a*. Isosbestic points at 223.5 and 244 nm remain at the initial step of the process (curves *1*—*4*), but they disappear upon further irradiation (see Fig. 2, *a*, curve *5*). The photoreduction products,[48] $Pt^{II}$ complexes, display no noticeable absorption in the region of >230 nm. Therefore, the behavior of isosbestic points suggests that photosolvation is mainly observed at the first step of photolysis, *i.e.*, the quantum yield of photosolvation is significantly higher than that of photoreduction.

The quantum yield for the first process step was calculated on the hypothesis that phosolvation affords $Pt^{IV}Cl_5(CH_3OH)^-$, which does not absorb at 265 nm (the maximum of $Pt^{IV}Cl_6^{2-}$ absorption band in methanol). This

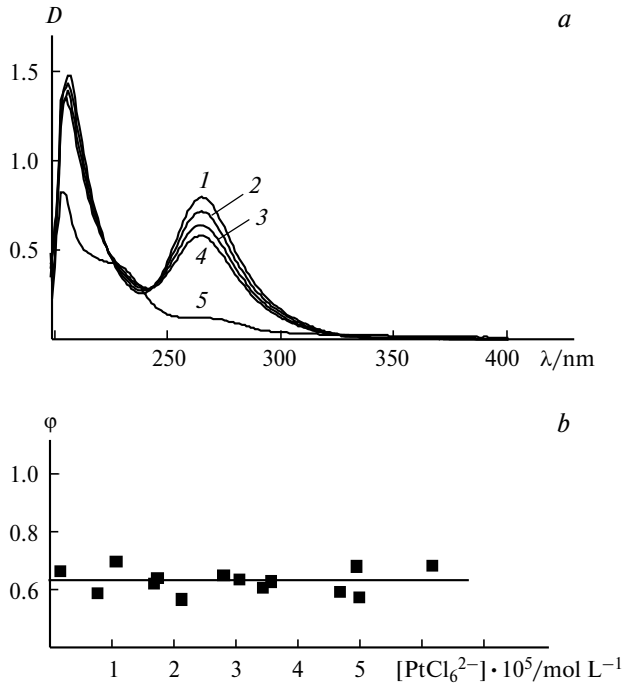


**Fig. 2.** Spectral changes (1 cm cell, natural level of oxygen) during photolysis (282 nm) of the $PtCl_6^{2-}$ complex ($3.4 \cdot 10^{-5}$ mol $L^{-1}$) in methanol (*a*): irradiation for 0 (*1*), 5 (*2*), 10 (*3*), 15 (*4*), and 90 s (*5*). The quantum yield of photosolvation *vs.* the starting complex concentration (*b*) (irradiation at 313 nm); the quantum yield was calculated assuming that the solvation product $Pt^{IV}Cl_5(CH_3OH)^-$ does not absorb at 265 nm.

assumption gives a lower-bound estimate of quantum yield. The quantum yield of photosolvation does not depend on the concentration of starting complex (see Fig. 2, *b*) to be $\varphi_{solv}^{313} \geq 0.63 \pm 0.07$ at $\lambda = 313$ nm. The independence of quantum yield on the concentration of starting complex contradicts the statement[46] of that the process proceeds by the chain mechanism. The lower-bound estimate of photosolvation quantum yield at $\lambda = 405$ nm is significantly lower to be $\varphi_{solv}^{405} \geq 0.1$.

The first steps of $Pt^{IV}Cl_6^{2-}$ photoreduction in simple alcohols at $\lambda = 308$ nm were studied in Refs 49, 59, and 60 by the nanosecond laser pulsed photolysis. The reduction of $Pt^{IV}$ was initiated by the outer-sphere electron transfer from the solvent molecule to the light-excited complex to form $Pt^{III}Cl_6^{3-}$ and hydroxyalkyl radical.[60] The mechanism of photolysis for a solution of $Pt^{IV}Cl_6^{2-}$ in methanol is represented by Eqs (12)—(16). The $Pt^{III}Cl_6^{3-}$ complex dissociates into $Pt^{III}Cl_5^{2-}$ and $Cl^-$ ions (see reaction (14); the process proceeds both thermally and photochemically.[49] The $Pt^{III}Cl_5^{2-}$ intermediate also dissociates to form a relatively long-living $Pt^{III}Cl_4^-$ complex. The final product of photolysis is the $Pt^{II}Cl_4^{2-}$ complex. The hydroxymethyl radicals as in the case of bromide complexes do not react with platinum complexes of any valence at measurable rate constants.[59]

$$Pt^{IV}Cl_6^{2-} \overset{h\nu}{\rightleftharpoons} (Pt^{IV}Cl_6^{2-})^* \quad (12)$$

$$(Pt^{IV}Cl_6^{2-})^* \xrightarrow{CH_3OH} Pt^{III}Cl_6^{3-} + {}^{\bullet}CH_2OH + H^+ \quad (13)$$

$$Pt^{III}Cl_6^{3-} \xrightarrow{t^\circ,\ h\nu} Pt^{III}Cl_5^{2-} + Cl^- \quad (14)$$

$$Pt^{III}Cl_5^{2-} \longrightarrow Pt^{III}Cl_4^- + Cl^- \quad (15)$$

$$Pt^{III}Cl_4^- + CH_3OH \longrightarrow Pt^{II}Cl_4^{2-} + {}^{\bullet}CH_2OH + H^+ \quad (16)$$

The mechanism of reactions (12)—(16) was confirmed by ESR detection of hydroxymethyl radicals upon photolysis of $Pt^{IV}Cl_6^{2-}$ in frozen alcohol matrices (both directly[61] and using spin traps[62]). Specific intermediates complicating the scheme of photolysis represented by reactions (12)—(16) are $Pt^{III}$ complexes with hydroalkyl radicals.[59,60]

Based on the results from the steady-state photolysis (the quantum yield is independent of the starting complex concentration) and laser flash photolysis (the $Pt^{III}$ intermediate emerges in the primary photochemical process), one can conclude that photosolvation and photoreduction of $Pt^{IV}Cl_6^{2-}$ in alcohols are concurrent photochemical processes.

**Processing of the experimental data from ultrafast kinetic spectroscopy.** Let us describe data obtained for solutions of the $Pt^{IV}Br_6^{2-}$ and $Pt^{IV}Cl_6^{2-}$ complexes by ultrafast kinetic spectroscopy upon near-UV excitation (320 nm). The experimental curves were fitted with the three-exponential function (17):

$$\Delta D(\lambda,t) = A_1(\lambda)\exp(-k_1 t) + A_2(\lambda)\exp(-k_2 t) + A_3(\lambda)\exp(-k_3 t). \quad (17)$$

The results of global fit and presumed correlation of observed times with elementary photophysical and photochemical processes are given in Table 2.

Fitting of the resulting data with function (17) contemplates (see Table 2) successive transformation of intermediates (according to the scheme $1 \rightarrow 2 \rightarrow 3 \rightarrow$ ground state + products which do not absorb in the detection wavelength range). The differential absorption spectra corresponding to particular components of this transformation chain (Species Associated Difference Spectra, SADS) were calculated by the formulas[63]

$$S_1(\lambda) = A_1(\lambda) + A_2(\lambda) + A_3(\lambda), \quad (18)$$

$$S_2(\lambda) = A_2(\lambda)(k_1 - k_2)/k_1 + A_3(\lambda)(k_1 - k_3)/k_1, \quad (19)$$

$$S_3(\lambda) = A_3(\lambda)(k_1 - k_3)(k_2 - k_3)/(k_1 k_2). \quad (20)$$

Note that $S_1(\lambda)$, $S_2(\lambda)$, and $S_3(\lambda)$ virtually coincide with the amplitudes of individual components $A_1(\lambda)$, $A_2(\lambda)$, and $A_3(\lambda)$ at a great difference between the rate constants (hereafter, the $\lambda$ argument was omitted upon record of SADS).

**Primary photoprocesses for the $PtBr_6^{2-}$ complex.** The examples of kinetic curves for aqueous solutions of the $Pt^{IV}Br_6^{2-}$ complex are given in Fig. 3. The processes at all wavelengths are completed in ~50 ps. The initial segments of kinetic curves ($t < 0.8$ ps, see Fig. 3, *b*) display a coherent artifact caused by the coherent interaction between exciting and probing pulses.[64] The value of coherent artifact depends, particularly, on the laser excitation wavelength. In the experiments[10,33,36] performed upon excitations at 400—420 nm, the coherent artifact was so low that it did not interfere with kinetic curve fitting. Upon excitation at 320 nm, the coherent artifact allowed no correct determination of spectral and kinetic parameters of intermediates emerging within the first picosecond after laser pulse. Upon fitting of the kinetic curves (see Fig. 3), the points with delay times of >0.5 ps were excluded.

Figure 4 shows the SADS of $Pt^{IV}Br_6^{2-}$ aqueous solutions obtained upon fitting of the kinetic curves in Fig. 3 by formulas (17)—(20). The results of fitting are given in Table 2. For reference, Table 2 gives the published data corresponding to excitation of the complex in the visible spectral range. In all cases, satisfactory processing of the

**Table 2.** Data from ultrafast kinetic spectroscopy on $Pt^{IV}$ halogenated complexes in water and methanol

| Complex, solvent | $\tau_1$/ps | Process | $\tau_2$/ps | Process | $\tau_3$/ps | Process |
|---|---|---|---|---|---|---|
| | | | Excitation at 405—420 nm* | | | |
| $PtBr_6^{2-}$, $H_2O$ | 0.4 | $(PtBr_6^{2-})^* \rightarrow$ $\rightarrow {}^3PtBr_5^- + Br^-$ | 2.2 | ${}^3PtBr_5^- \rightarrow$ $\rightarrow {}^1PtBr_5^-$ | 15 | ${}^1PtBr_5^- \rightarrow PtBr_6^{2-}$, ${}^1PtBr_5^- \rightarrow PtBr_5(H_2O)^-$ |
| $PtBr_6^{2-}$, $CH_3OH$ | 1.3±0.3 | ${}^3PtBr_5^- \rightarrow {}^1PtBr_5^-$, ${}^3PtBr_5^- + CH_3OH \rightarrow$ $\rightarrow {}^2PtBr_5^{2-}$ | 8.7 | ${}^1PtBr_5^- + Br^- \rightarrow$ $\rightarrow PtBr_6^{2-}$, ${}^1PtBr_5^- +$ $+ CH_3OH \rightarrow$ $\rightarrow PtBr_5(CH_3OH)^-$ | 130 | ${}^2PtBr_5^{2-} + CH_3OH \rightarrow$ $\rightarrow PtBr_4^{2-}$ + products |
| $PtCl_6^{2-}$, $H_2O$ | 0.6±0.02 | $PtCl_6^{2-}$ ${}^3(T_{1g} + T_{2g}) \rightarrow \mathbf{A}^*$ | 8.6 | $\mathbf{A}^* \rightarrow \mathbf{A}$ | 220 | Transition to ground-state and formation of products |
| $PtCl_6^{2-}$, $CH_3OH$ | 0.7±0.1 | | 4.3 | | 350 | |
| | | | Excitation at 320 nm | | | |
| $PtBr_6^{2-}$, $H_2O$ | 0.3±0.1 | $(PtBr_6^{2-})^* \rightarrow$ $\rightarrow {}^3PtBr_5^- + Br^-$ | 2.6±0.2 | ${}^3PtBr_5^- \rightarrow$ $\rightarrow {}^1PtBr_5^-$ | 14.5±0.3 | ${}^1PtBr_5^- \rightarrow PtBr_6^{2-}$ ${}^1PtBr_5^- \rightarrow$ $\rightarrow PtBr_5(H_2O)^-$ |
| $PtBr_6^{2-}$, $CH_3OH$ | 2.0±0.5 | ${}^3PtBr_5^- \rightarrow {}^1PtBr_5^-$, ${}^3PtBr_5^- +$ $+ CH_3OH \rightarrow$ $\rightarrow {}^2PtBr_5^{2-}$ | 10.3±1.0 | ${}^1PtBr_5^- + Br^- \rightarrow$ $\rightarrow PtBr_6^{2-}$, ${}^1PtBr_5^- +$ $+ CH_3OH \rightarrow$ $\rightarrow PtBr_5(CH_3OH)^-$ | 118±16 | ${}^2PtBr_5^{2-} +$ $+ CH_3OH \rightarrow$ $\rightarrow PtBr_4^{2-} +$ + products |
| $PtCl_6^{2-}$, $H_2O$ | 0.6±0.1 | $PtCl_6^{2-}$ ${}^{1,3}(T_{1u} + T_{2u}) \rightarrow$ $\rightarrow \mathbf{A}^*$ | 6.2±1.0 | $\mathbf{A}^* \rightarrow \mathbf{A}$ | 180±40 | Transition to ground-state and formation of products |
| $PtCl_6^{2-}$, $CH_3OH$ | 0.4±0.2 | | 6.7±2.5 | | ~200 | |

* According to the data for $PtBr_6^{2-}$ in $H_2O$,[33] $PtBr_6^{2-}$ and $PtCl_6^{2-}$ in $CH_3OH$,[10] and $PtCl_6^{2-}$ in $H_2O$.[10,36]

kinetic data required the three-exponential fit (17); however, the presence of coherent artifact made it impossible to determine reliably the initial spectrum of intermediate absorption and the shortest characteristic time.

For this reason, the starting spectrum of intermediate absorption (see Fig. 4, curve $S_1$) with maxima at 470—530 and 600 nm does not correspond to the initial Franck—Condon state. It corresponds to the product of the Franck—Condon state transformation for several hundreds femtoseconds. In fact (except for small proportional changes in the absorbance), the SADS $S_1$ and $S_2$ coincide. Then, a band with an absorption maximum at 420—450 nm forms with a charactetistic time of ~3 ps; the corresponding SADS is represented by the curve $S_3$ in Fig. 4. In general, the spectral changes observed after laser pulse and their interpretations are analogous to those proposed for the photolysis at 400—420 nm (see Table 2). The scheme of processes observed is represented by Eqs (21)—(26).

$$Pt^{IV}Br_6^{2-}({}^1A_{1g}) \xrightarrow{h\nu} Pt^{IV}Br_6^{2-}(1{}^1T_{1u}{}^*,\ 2{}^1T_{1u}{}^*), \qquad (21)$$

$$Pt^{IV}Br_6^{2-}(1{}^1T_{1u}{}^*,\ 2{}^1T_{1u}{}^*) \longrightarrow Pt^{IV}Br_6^{2-}({}^3T_{1g}{}^*), \qquad (22)$$

$$Pt^{IV}Br_6^{2-}({}^3T_{1g}{}^*) \longrightarrow \{{}^3Pt^{IV}Br_5^- + Br^-\}_{cage}, \qquad (23)$$

$$\{{}^3Pt^{IV}Br_5^- + Br^-\}_{cage} \longrightarrow \{{}^1Pt^{IV}Br_5^- + Br^-\}_{cage}, \qquad (24)$$

$$\{{}^1Pt^{IV}Br_5^- + Br^-\}_{cage} \longrightarrow Pt^{IV}Br_6^{2-}({}^1A_{1g}), \qquad (25)$$

$$\{{}^1Pt^{IV}Br_5^- + Br^-\}_{cage} + H_2O \longrightarrow Pt^{IV}Br_5^-(H_2O) + Br^-. \qquad (26)$$

Equations (21)—(26) suggest the independence of the photoaquation quantum yield on the excitation wavelength. Except for the reactions which were not observed in our experiment (see Eqs (21) and (22)), the remaining reactions coincide with those given in Ref. 36 for photolysis of the $Pt^{IV}Br_6^{2-}$ complex at 400—420 nm. The dissociative nature of the lowest excited triplet state of $Pt^{IV}Br_6^{2-}$

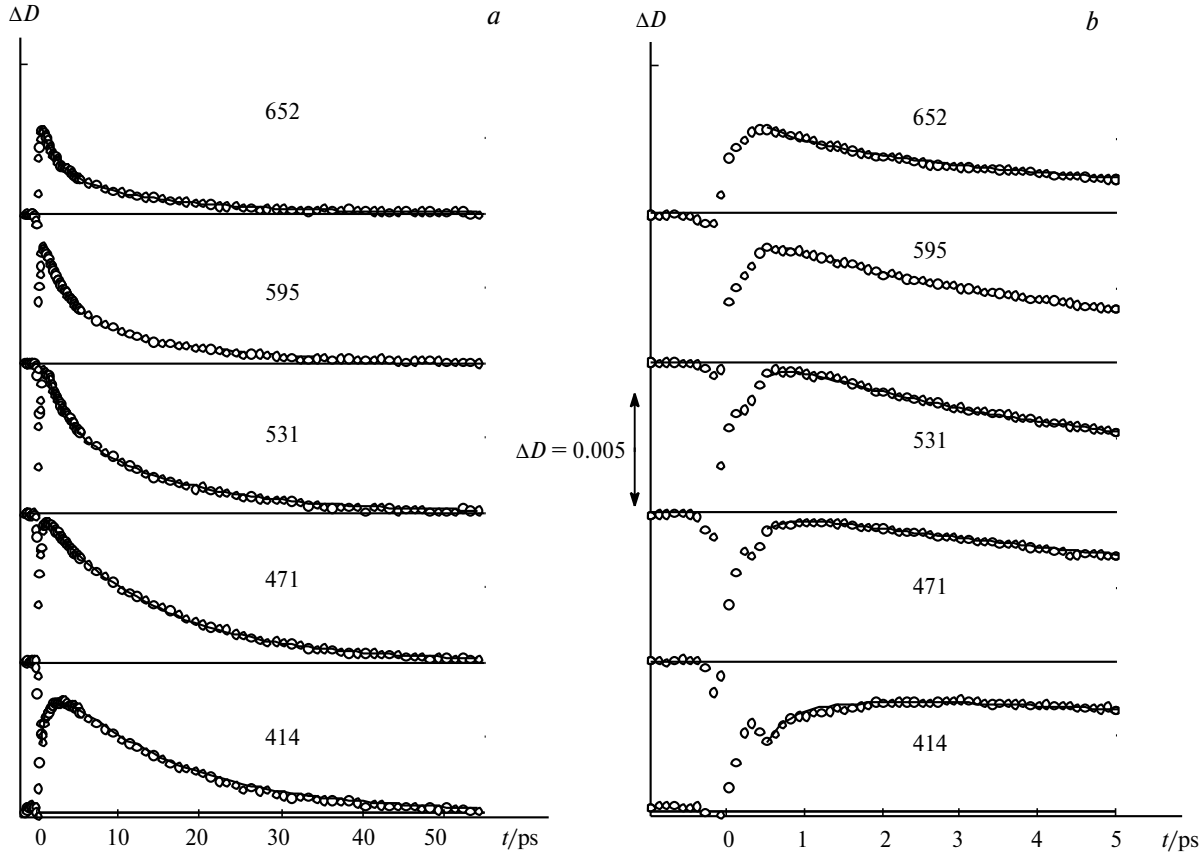


**Fig. 3.** Kinetic curves (*a*, *b*) for intermediate absorption in the experiments on ultrafast kinetic spectroscopy of the $PtBr_6^{2-}$ complex in water ($\lambda_{exc}$ = 320 nm, $2.2 \cdot 10^{-4}$ mol $L^{-1}$). The cell thickness is 1 mm. The points are experimental data and the solid lines are the global fits of experimental curves with the three-exponential function after convolution with the response function. Here and in Fig. 5, the numbers near curves indicate $\lambda_{exc}$/nm.

($^3T_{1g}$) has been proved earlier.[34] The intermediates are five-coordinated $Pt^{IV}$ complexes.[34,35] The observed spectra of intermediate absorption (see Fig. 4, Table 2) are interpreted quite simply: curve $S_2$ belongs to the $Pt^{IV}Br_5^-$ complex with a symmetry close to $D_{3h}$ whose ground state is triplet and curve $S_3$ belongs to the same-composition complex with a $C_{4v}$ symmetry (the ground state is singlet). Thus, upon photoexcitation of aqueous solutions of the $Pt^{IV}Br_6^{2-}$ complex, a fast (with a characteristic time of 15 ps) photoaquation occurs by the heterolytic mechanism regardless of the excitation wavelength.

The kinetic curves and SADS emerging upon photolysis of the $Pt^{IV}Br_6^{2-}$ complex in methanol are shown in Figs 5 and 6, respectively. The processing data together with interpretation of the processes observed are given in Table 2.

The photolysis of $Pt^{IV}Br_6^{2-}$ in alcoholic solutions features the formation of a relatively long-living (>100 ps, see Fig. 5) SADS $S_3$ (see Fig. 6) with a maximum at 480 nm. The starting spectrum (SADS $S_1$) belongs to the triplet state of the $^3Pt^{IV}Br_5^-$ complex. The spectral changes for the first 150—200 fs unresolved in the described experiment reflect several processes: (I) internal conver-

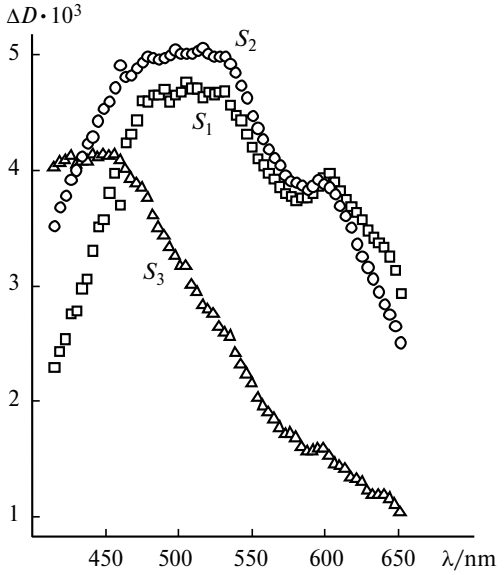


**Fig. 4.** Differential spectra of intermediates (SADS) emerging during the ultrafast kinetic spectroscopy study of $PtBr_6^{2-}$ complex in water ($\lambda_{exc}$ = 320 nm, $2.2 \cdot 10^{-4}$ mol $L^{-1}$). The cell thickness is 1 mm. The spectra were obtained by processing of the experimental data (see Fig. 3) by formulas (17)—(20).

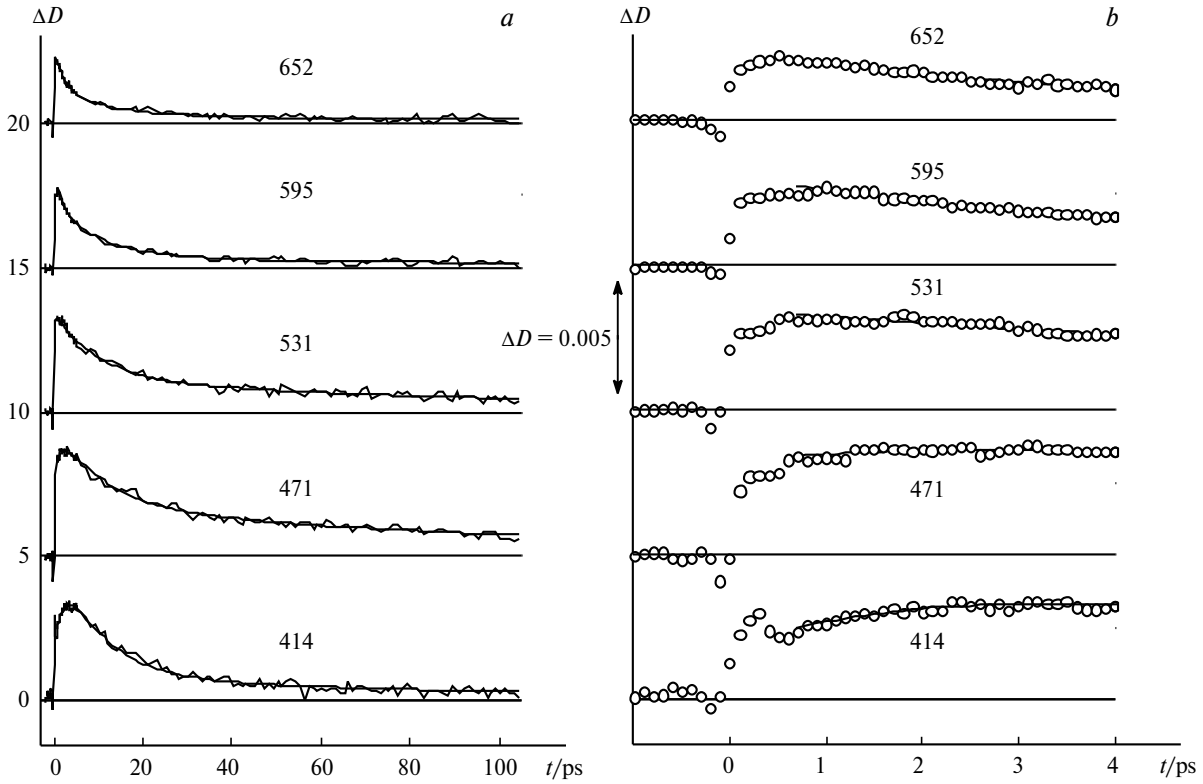


**Fig. 5.** Kinetic curves for intermediate absorption in the experiments on ultrafast kinetic spectroscopy of the $PtBr_6^{2-}$ complex in methanol ($\lambda_{exc}$ = 320 nm, $2.7 \cdot 10^{-4}$ mol $L^{-1}$). The cell thickness is 1 mm. The zigzag lines (*a*) and points (*b*) are experimental data and the solid lines are the global fits of experimental curves with the three-exponential function after convolution with the response function.

sion, (II) intercombination conversion of $Pt^{IV}Br_6^{2-}$ to the lowest dissociative $^3T_{1g}$ triplet excited state, (III) loss of ligand to form the triplet product $^3Pt^{IV}Br_5^-$, which then is involved in concurrent processes: (IV) it transits into the singlet state $^1Pt^{IV}Br_5^-$, (V) transfers an electron from the solvent molecule or (VI) from the hydroxyalkyl radical formed in the previous process to result in the $Pt^{III}$ intermediate. Processes (I)—(IV) are analogous to those proceeding in aqueous solutions and processes (V) and (VI) are specific to alcohols. Within ~10 ps, the $^1Pt^{IV}Br^{5-}$ complex recombines with the $Br^-$ anion in the solvent cage and undergoes solvation to form the $Pt^{IV}Br_5(CH_3OH)^-$ complex. The spectrum $S_3$ (see Fig. 6) belongs to the $^2Pt^{III}Br_5^{2-}$ complex. The electron transfer from the solvent molecule to this intermediate results in the final photoreduction product,[10] a planar $Pt^{II}Br_4^{2-}$ complex.

Thus, concurrent reactions, photosolvation and photoreduction, proceed upon photoexcitation of $Pt^{IV}Br_6^{2-}$ in simple alcohols. The detailed mechanism for the photolysis of $Pt^{IV}Br_6^{2-}$ in alcoholic solutions includes reactions (21)—(26) as in the case of aqueous solutions and reactions (27)—(30):

$$\{^1Pt^{IV}Br_5^- + Br^-\}_{cage} + CH_3OH \longrightarrow Pt^{IV}Br_5(CH_3OH)^- + Br^-, \quad (27)$$

$$\{^3Pt^{IV}Br_5^-...Br^-\}_{cage} + CH_3OH \longrightarrow Pt^{III}Br_5^{2-} + {}^{\cdot}CH_2OH + H^+ + Br^-, \quad (28)$$

$$Pt^{III}Br_5^{2-} + CH_3OH \longrightarrow Pt^{II}Br_4^{2-} + {}^{\cdot}CH_2OH + H^+ + Br^-, \quad (29)$$

$$Pt^{III}Br_5^{2-} + {}^{\cdot}CH_2OH \longrightarrow Pt^{II}Br_4^{2-} + CH_2O + H^+ + Br^-. \quad (30)$$

The results obtained in the present work for photolysis of the $Pt^{IV}Br_6^{2-}$ complex in methanol are analogous to those considered[10] for excitation at 420 nm. The same pattern was observed for aqueous solutions. Meanwhile, irradiation at 320 nm excites an intense charge transfer band and irradiation at 400—420 nm corresponds to the region of intersection between the less intense LMCT transition and the d—d transition (see Fig. 1, Table 1). In all cases, a fast intercombination conversion results in the formation of the $^3T_{1g}$ lowest electronic excited state of the starting complex, which is dissociative. Therefore, the photochemical behavior of the $Pt^{IV}Br_6^{2-}$ complex upon excitation at different wavelengths is identical. The difference in the photophysical processes corresponding to

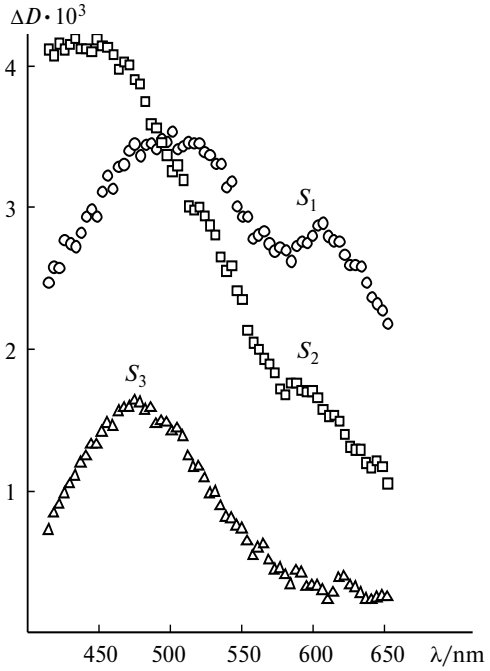


**Fig. 6.** Differential spectra of intermediates (SADS) emerging during the ultrafast kinetic spectroscopy study of $PtBr_6^{2-}$ complex in methanol ($\lambda_{exc}$ = 320 nm, $2.7 \cdot 10^{-4}$ mol $L^{-1}$). The cell thickness is 1 mm. The spectra were obtained by processing of the experimental data (see Fig. 5) by formulas (17)—(20).

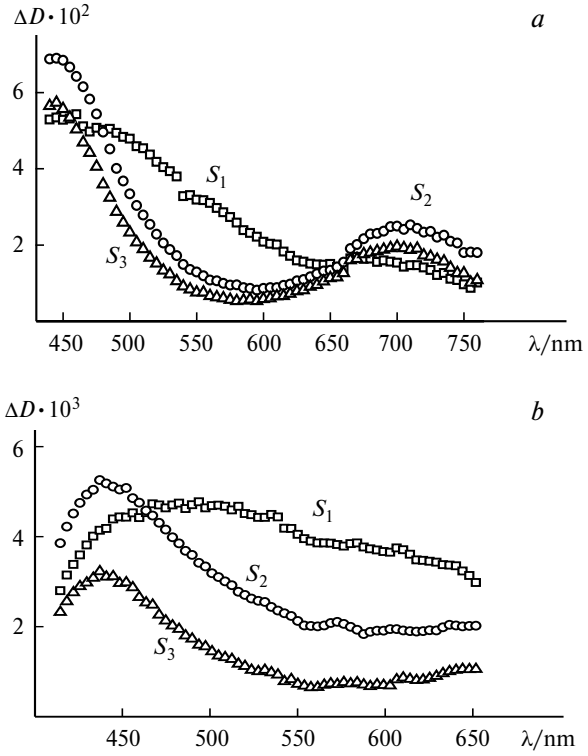


**Fig. 7.** Differential spectra of intermediates (SADS) emerging during the ultrafast kinetic spectroscopy study of $PtCl_6^{2-}$ complex in water. The spectra were obtained by processing of the experimental data by formulas (17)—(20): (*a*) $\lambda_{exc}$ = 405 nm, the concentration is 0.03 mol $L^{-1}$, the cell thickness is 1 mm (the experimental data from Ref. 18); (*b*) $\lambda_{exc}$ = 320 nm, the concentration is $2.4 \cdot 10^{-3}$ mol $L^{-1}$, the cell thickness is 1 mm.

different absorption bands can be manifested only within the first several hundreds femtoseconds after laser pulse.

**Primary photoprocesses for the $Pt^{IV}Cl_6^{2-}$ complex.** Irradiation of the $Pt^{IV}Cl_6^{2-}$ at $\lambda$ = 405 nm (d—d transitions) affords[47] the triplet excited states with $^3T_{1g}$ and $^3T_{2g}$ symmetries. The emission at 320 nm corresponds to intersection between the long-wave wing of the charge transfer band with a maximum at 263 nm and the d—d bands, the contribution of the latter seems to be not more than 20% (see Fig. 1). The LMCT transitions result in the formation of excited states with the $^1T_{1u}$, $^3T_{1u}$, $^1T_{2u}$, and $^3T_{2u}$ symmetries and the d—d transitions contribute to the emergence of $^1T_{1g}$ and $^3T_{2g}$ states.[46] Accordingly, one can expect a significant difference in the intermediate absorption spectra emerging immediately after femtosecond laser irradiation at 405 and 320 nm.

For aqueous solutions of $Pt^{IV}Cl_6^{2-}$, the kinetic curves for excitation at 320 and 405 nm (in the latter case, the data from Ref. 10 were used) are satisfactorily fitted with the three-exponential function (17). The corresponding SADS are shown in Fig. 7 (the spectral detection regions in two experiments differ slightly) and their interpretations are given in Table 2. Upon photolysis at 320 nm, despite the presence of coherent artifact, we succeeded to record the spectrum of the starting intermediate. As shown above, the spectra of these intermediates (curves $S_1$ in Fig. 7, *a* and *b*) corresponding to excitations in the regions of charge transfer and d—d bands differ significantly. The starting intermediate transforms into another species which is the same in both cases. In Refs 10 and 36, this intermediate was designated as intermediate **A**. It has two characteristic absorption bands with maxima at ~440 and 700 nm and has lifetime of ~200 ps (in the experiments with excitation at 320 nm, for technical reasons only one short-wave region of the spectrum of second band was recorded). The disappearance of intermediate **A** results in the formation of products which do not absorb in the available spectral range. The spectra $S_2$ and $S_3$ in Fig. 7 correspond to the vibrationally excited and relaxed states of intermediate **A**. The coincidence of intermediates emerging upon excitation at different wavelengths suggests a similarity of photochemical processes.

In Ref. 10, intermediate **A** was interpreted as the primary radical pair $[Pt^{III}Cl_5^{2-}(C_{4v})...Cl^{\bullet}]$ being a key participant in the Adamson redox mechanism of photoaquation[32] (for such species, the term "Adamson radical pair" is conventionally used, although what is meant here is the pair radical—metal ion in unusual oxidation state). The scheme of reactions proceeding within a time of <1 ns is represented by Eqs (31)—(36):

$$Pt^{IV}Cl_6^{2-} \xrightleftharpoons{h\nu} (Pt^{IV}Cl_6^{2-})^*, \quad (31)$$

$$(Pt^{IV}Cl_6^{2-})^* \longrightarrow [Pt^{III}Cl_5^{2-}(C_{4v})...Cl^{\bullet}], \quad (32)$$

**A**

$$[Pt^{III}Cl_5^{2-}(C_{4v})...Cl^{\bullet}] \longrightarrow Pt^{IV}Cl_6^{2-}, \quad (33)$$

$$[Pt^{III}Cl_5^{2-}(C_{4v})...Cl^{\bullet}] + H_2O \longrightarrow$$

$$\longrightarrow [Pt^{III}Cl_5(H_2O)^{2-}...Cl^{\bullet}], \quad (34)$$

**RP**

$$[Pt^{III}Cl_5(H_2O)^{2-}...Cl^{\bullet}] \longrightarrow$$

$$\longrightarrow Pt^{IV}Cl_5(H_2O)^- + Cl^-, \quad (35)$$

$$[Pt^{III}Cl_5(H_2O)^{2-}...Cl^{\bullet}] \longrightarrow$$

$$\longrightarrow Pt^{III}Cl_5^{2-}(D_{3h}) + Cl^{\bullet} + H_2O, \quad (36)$$

**B**

where **A** and **B** are intermediates, **A** is the primary radical pair, and **RP** is the secondary radical pair.

Equations (31)—(36), besides the spectrally observed intermediate **A**, include intermediate **B** being inapparent in the spectral range available for measurements. Introduction of intermediate **B** makes the ultrafast steps of photochemical process consistent with subsequent reactions proceeding with characteristic times of >>1 ns. These reactions are represented by Eqs (6)—(11). The spectral characteristics of contemplated $Pt^{III}$ intermediates agree with the data from quantum chemical calculations.[7,55—57]

In general, the scheme of reactions (31)—(36) supplemented with Eqs (6)—(11) coincides with that proposed in Refs 10 and 36. The difference consists in reactions (31) and (32): irradiation in the regions of charge transfer band (320 nm, present work) and d—d transitions (405 nm)[10,36] results in the formation of different electronic excited states. However, these states afford the same intermediate **A**, as a result of which subsequent intermediates and final products are identical. The dependence of the quantum yield on the radiation wavelength is defined by the relative yield of intermediate **A** in reactions (31) and (32).

The differential spectra of intermediates (SADS) resulting from the three-exponential fit of the kinetic curves of intermediate absorption obtained upon irradiation of the $Pt^{IV}Cl_6^{2-}$ complex in methanol at 405 (see Ref. 10) and 320 nm are shown in Fig. 8. The measured rate constants and their interpretations are given in Table 2. As in the case of aqueous solutions, the spectra of starting intermediates corresponding to excitation in the regions of charge transfer and d—d transitions (curves $S_1$ in Fig. 8, *a* and *b*) differ significantly. The excited states transform

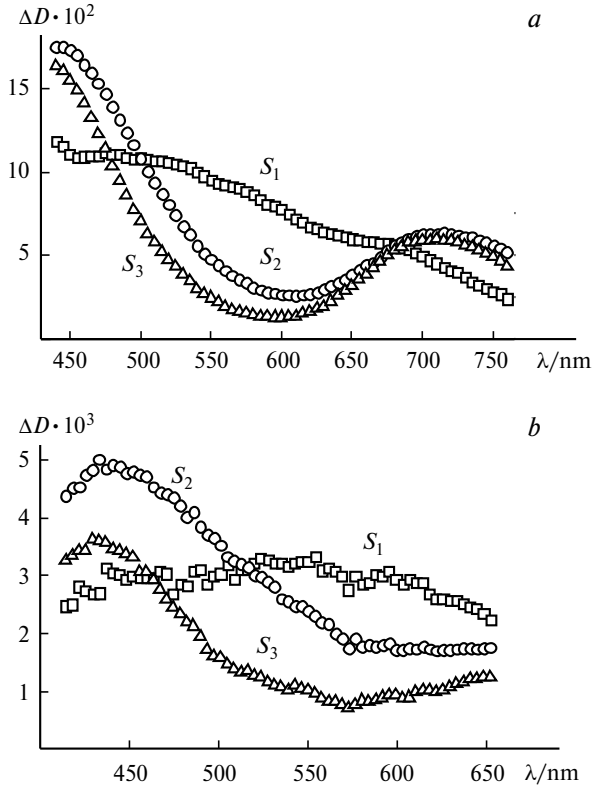


**Fig. 8.** Differential spectra of intermediates (SADS) emerging during the ultrafast kinetic spectroscopy study of $PtCl_6^{2-}$ complex in methanol. The spectra were obtained by processing of the experimental data by formulas (17)—(20): (*a*) $\lambda_{exc}$ = 405 nm, the concentration is 0.052 mol $L^{-1}$, the cell thickness is 1 mm (experimental data from Ref. 18); (*b*) $\lambda_{exc}$ = 320 nm, the concentration is $2.7 \cdot 10^{-3}$ mol $L^{-1}$, the cell thickness is 1 mm.

into the same intermediate **A** (curves $S_3$ in Fig. 8, *a* and *b*) interpreted as the primary Adamson radical pair $[Pt^{III}Cl_5^{2-}(C_{4v})...Cl^{\bullet}]$, which transforms into the reaction products. One should note nearly two-fold difference between its decay times (see Table 2) upon excitation at 405 nm (350 ps, see Ref. 10) and at 320 nm (200 ps, present work). The only acceptable explanation of this difference is insufficient length of the time range used for detection of intermediate absorption. The value of $\tau_3 \approx 200$ ps should be regarded as an estimate.

The full scheme of photoprocesses for the $Pt^{IV}Cl_6^{2-}$ complex in methanol includes reactions (31)—(33) analogous to those proceeding in aqueous solutions followed by transformation of the Adamson radical pair into photosolvation and photoreduction products:

$$[Pt^{III}Cl_5^{2-}(C_{4v})...Cl^{\bullet}] + CH_3OH \longrightarrow$$

$$\longrightarrow Pt^{IV}Cl_5(CH_3OH)^- + Cl^-, \quad (37)$$

$$[Pt^{III}Cl_5^{2-}(C_{4v})...Cl^{\bullet}] + CH_3OH \longrightarrow$$

$$\longrightarrow Pt^{III}Cl_6^{3-} + {}^{\bullet}CH_2OH + H^+. \quad (38)$$

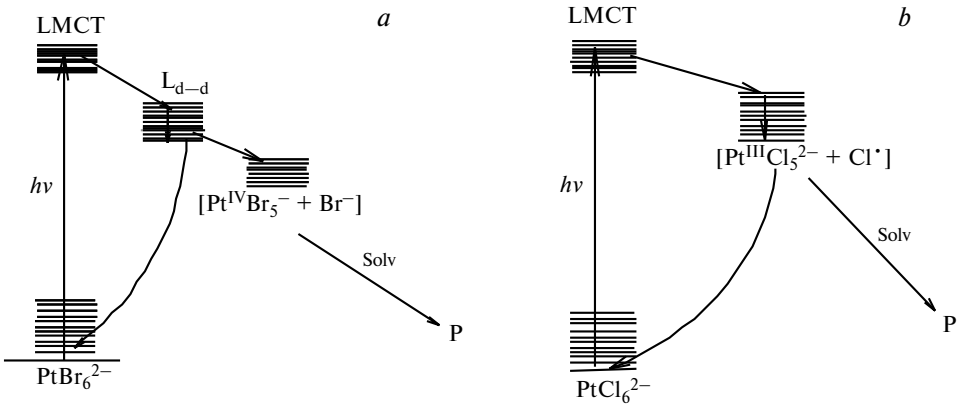


**Fig. 9.** General view of the Jablonski diagrams for the photolysis of $PtBr_6^{2-}$ (*a*) and $PtCl_6^{2-}$ (*b*) in water and methanol; $L_{d-d}$ is the lowest d—d excited state, Solv is solvent, and P are products.

Subsequent processes occurring in the nano- and microsecond time ranges result in the reduction of Pt atom to the divalent state and are described[59—61] by Eqs (14)—(16).

**Comparison between the photoexcitation data for the $Pt^{IV}Br_6^{2-}$ and $Pt^{IV}Cl_6^{2-}$ complexes in different spectral ranges.** The present work gives the data from ultrafast kinetic spectroscopy of aqueous and methanol solutions of the $Pt^{IV}Br_6^{2-}$ and $Pt^{IV}Cl_6^{2-}$ complexes upon excitation in the band region of charge transfer from the ligand-centered group π-orbitals to the $e_g$*-orbital of complex anion. The data obtained earlier[10,33,36] upon excitation in the region of d—d bands were compared. No fundamental difference related to excitation of other electron transitions was found. The processes are described by the Jablonski diagrams shown in Fig. 9. The photochemical properties of complexes are caused by the reactions of key intermediates formed independently of the excitation wavelength, *viz.*, $Pt^{IV}Br_5^-$ complex and the Adamson radical pair $[Pt^{III}Cl_5^{2-}(C_{4v})...Cl^\bullet]$ for $Pt^{IV}Br_6^{2-}$ and $Pt^{IV}Cl_6^{2-}$, respectively. The difference in the exciting light wavelengths has an impact only on the first process step, *i.e.*, transition from the Franck—Condon excited state to the reaction intermediates. Note also that the assignment of the key intermediate **A** emerging upon photolysis of the $Pt^{IV}Cl_6^{2-}$ complex to the Adamson radical pair requires additional quantum chemical calculations.

This work was financially supported by the Russian Foundation for Basic Research (Project No. 14-03-00692-a) and the Russian Scientific Foundation (Grant 15-13-10012).

## References

1. J. Hershel, *Phil. Mag.*, 1832, **1**, 58.
2. V. Balzani, V. Carassiti, in *Photochemistry of Coordination Compounds*, Acad. Press, New York, 1970, 257—269, 307—312.
3. P. G. Ford, J. D. Petersen, R. E. Hintze, *Coord. Chem. Rev.*, 1974, **14**, 67.
4. *Concepts of Inorganic Photochemistry*, Eds A. W. Adamson, P. D. Fleischauer, Wiley, New York, 1975, 439 pp.
5. J. Sykora, J. Sima, *Photochemistry of Coordination Compounds*, Elsevier, Amsterdam—Oxford—New York—Tokio, 1990, 225 pp.
6. R. C. Wright, G. S. Laurence, *J. Chem. Soc., Chem. Commun.*, 1972, 132.
7. A. Goursot, A. D. Kirk, W. L. Waltz, G. B. Porter, D. K. Sharma, *Inorg. Chem.*, 1987, **26**, 14.
8. W. L. Waltz, J. Lillie, A. Goursot, H. Chermette, *Inorg. Chem.*, 1989, **28**, 2247.
9. I. V. Znakovskaya, Yu. A. Sosedova, E. M. Glebov, V. P. Grivin, V. F. Plyusnin, *Photochem. Photobiol. Sci.*, 2005, **4**, 897.
10. E. M. Glebov, A. V. Kolomeets, I. P. Pozdnyakov, V. F. Plyusnin, V. P. Grivin, N. V. Tkachenko, H. Lemmetyinen, *RSC Adv.*, 2012, **2**, 5768.
11. L. E. Cox, D. G. Peters, E. L. Wehry, *J. Inorg. Nucl. Chem.*, 1972, **14**, 297.
12. K. P. Balashev, V. V. Vasil´ev, A. M. Zimnyakov, G. A. Shagisultanova, *Koord. Khim.*, 1984, **10**, 976 [*Sov. J. Coord. Chem.* (*Engl. Transl.*), 1984, **10**].
13. R. E. Cameron, A. B. Bocarsly, *J. Am. Chem. Soc.*, 1985, **107**, 6116.
14. R. E. Cameron, A. B. Bocarsly, *Inorg. Chem.*, 1986, **25**, 2910.
15. M. Sakamoto, M. Fujistuka, T. Majima, *J. Photochem. Photobiol. C: Photochem. Rev.*, 2009, **10**, 33.
16. N. Toshima, T. Takahashi, *Bull. Chem. Soc. Jpn*, 1992, **65**, 400.
17. N. Toshima, K. Nakata, H. Kitoh, *Inorg. Chim. Acta*, 1997, **265**, 149.
18. H. Einaga, M. Harada, *Langmuir*, 2005, **21**, 2578.
19. M. Harada, K. Okamoto, M. Terazima, *Langmuir*, 2006, **22**, 9142.
20. M. Harada, H. Einaga, *Langmuir*, 2006, **22**, 2371.
21. Yu. Borodko, P. Ercius, D. Zherebetskyy, Y. Wang, Y. Sun, G. Somorjai, *J. Phys. Chem. C,* 2013, **117**, 26667.
22. H. Chang, Y. Tsai, C. Cheng, C. Lin, P. Wu, *J. Power Sources*, 2013, **239**, 164.
23. L. Zang, W. Macyk, C. Lange, W.F. Mayer, C. Antonius, D. Meissner, H. Kish, *Chem. Eur. J.*, 2000, **6**, 379.
24. W. Macyk, H. Kish, *Chem. Eur. J.*, 2001, **7**, 1862.
25. H. Kish, *Adv. Inorg. Chem.*, 2011, **63**, Ch. 9, 371.

26. F. Mahlamvana, R. J. Kriek, *Appl. Catal. B: Environ.*, 2014, **148—149**, 387.
27. Q. Li, Zh. Chen, X. Zheng, Zh. Jin, *J. Phys. Chem.*, 1992, **96**, 5959.
28. C. Harris, P. V. Kamat, *ACS Nano*, 2010, **4**, 7321.
29. K. L. Swancutt, S. P. Mezyk, J. J. Kiddle, *Radiat. Res.*, 2007, **168**, 423.
30. J. Pracharova, L. Zerzankova, J. Stepankova, O. Novakova, N. J. Farrer, P. J. Sadler, V. Brabec, J. Kasparkova, *Chem. Res. Toxicol.*, 2012, **25**, 1099.
31. N. Cutillas, G. C. Yellol, C. de Haro, C. Vicente, V. Rodriguez, J. Riuz, *Coord. Chem. Rev.*, 2013, **257**, 2784.
32. A. W. Adamson, A. H. Sporer, *J. Am. Chem. Soc.*, 1958, **80**, 3865.
33. I. P. Pozdnyakov, E. M. Glebov, V. F. Plyusnin, N. V. Tkachenko, H. Lemmetyinen, *Chem. Phys. Lett.*, 2007, **442**, 78.
34. I. L. Zheldakov, M. N. Ryazantsev, A. N. Tarnovsky, *J. Phys. Chem. Lett.*, 2011, **2**, 1540.
35. I. L. Zheldakov, Ph. D. Thesis, Bowling Green State University, 2010.
36. E. M. Glebov, A. V. Kolomeets, I. P. Pozdnyakov, V. P. Grivin, V. F. Plyusnin, N. V. Tkachenko, H. Lemmetyinen, *Russ. Chem. Bull.* (*Int. Ed.*), 2013, **62**, 1540 [*Izv. Akad. Nauk, Ser. Khim.*, 2013, 1540].
37. A. V. Litke, I. P. Pozdnyakov, E. M. Glebov, V. F. Plyusnin, N. V. Tkachenko, H. Lemmetyinen, *Chem. Phys. Lett.*, 2009, **477**, 304.
38. E. M. Glebov, A. V. Kolomeets, I. P. Pozdnyakov, V. F. Plyusnin, N. V. Tkachenko, H. Lemmetyinen, *Photochem. Photobiol. Sci.*, 2011, **10**, 1709.
39. E. M. Glebov, I. P. Pozdnyakov, A. A. Melnikov, S. V. Chekalin, *J. Photochem. Photobiol. A: Chem.*, 2014, **292**, 34.
40. C. Rensing, O. T. Ehrler, J.-P. Yang, A.-N. Unterreiner, M. M. Kappes, *J. Chem. Phys.*, 2009, **130**, 234306.
41. V. Balzani, M. F. Manfrin, L. Moggi, *Inorg. Chem.*, 1967, **6**, 354.
42. E. M. Glebov, V. F. Plyusnin, V. P. Grivin, A. B. Venediktov, S. V. Korenev, *Russ. Chem. Bull.* (*Int. Ed.*), 2007, **56**, 2357 [*Izv. Akad. Nauk, Ser. Khim.*, 2007, 2277].
43. S. V. Chekalin, *Phys. Usp.* (*Engl. Transl.*), 2006, **49**, 634 [*Usp. Fiz. Nauk*, 2006, **176**, 657].
44. *Sintez kompleksnykh soedinenii metallov platinovoi gruppy* [*Synthesis of Platinum-Group Metal Complexes*], Ed. I. I. Chernyaev, Nauka, Moscow, 1964, 339 pp.
45. C. K. Jorgensen, *Mol. Phys.*, 1959, **2**, 309.
46. K. R. Balashev, I. I. Blinov, G. A. Shagisultanova, *Koord. Khim.*, 1987, **13**, 1674 [*Sov. J. Coord. Chem.* (*Engl. Transl.*), 1987, **13**].
47. A. Goursot, E. Penigault, H. Chermette, *Chem. Phys. Lett.*, 1983, **97**, 215.
48. J. Chatt, G. A. Gamlen, L. E. Orgel, *J. Chem. Soc. Res.*, **1958**, 486—489.
49. V. P. Grivin, I. V. Khmelinski, V. F. Plyusnin, I. I. Blinov, K. P. Balashev, *J. Photochem. Photobiol. A: Chem.*, 1990, **51**, 167.
50. D. L. Swihart, W. R. Mason, *Inorg. Chem.*, 1970, **9**, 1749.
51. R. L. Rich, H. Taube, *J. Am. Chem. Soc.*, 1954, **76**, 2608.
52. L. E. Cox, D. G. Peters, E. L. Wehry, *J. Inorg. Nucl. Chem.*, 1972, **14**, 297.
53. R. C. Wright, G. S. Laurence, *J. Chem. Soc., Chem. Commun.*, 1972, 132.
54. K. R. Balashev, I. I. Blinov, G. A. Shagisultanova, *Zh. Neorg. Khim.*, 1987, **32**, 2470 [*J. Inorg. Chem. USSR* (*Engl. Transl.*), 1987, **32**].
55. W. L. Waltz, J. Lillie, A. Goursot, H. Chermette, *Inorg. Chem.*, 1989, **28**, 2247.
56. A. Goursot, H. Chermette, E. Peigault, M. Chanon, W. L. Waltz, *Inorg. Chem.*, 1984, **23**, 3618.
57. A. Goursot, H. Chermette, E. Peigault, M. Chanon, W. L. Waltz, *Inorg. Chem.*, 1985, **24**, 1042.
58. A. Goursot, H. Chermette, W. L. Waltz, J. Lillie, *Inorg. Chem.*, 1989, **28**, 2241.
59. V. P. Grivin, I. V. Khmelinski, V. F. Plyusnin, *J. Photochem. Photobiol. A: Chem.*, 1990, **51**, 379.
60. V. P. Grivin, I. V. Khmelinski, V. F. Plyusnin, *J. Photochem. Photobiol. A: Chem.*, 1991, **59**, 153.
61. G. A. Shagisultanova, *Koord. Khim.*, 1981, **7**, 1527 [*Sov. J. Coord. Chem.* (*Engl. Transl.*), 1981, **7**].
62. A. G. Fadnis, T. J. Kemp, *J. Chem. Soc. Dalton Trans.*, 1989, 1237.
63. A. S. Rury, R. J. Sension, *Chem. Phys.*, 2013, **422**, 220.
64. L. Palfrey, T. F. Heinz, *J. Opt. Soc. Am. B*, 1985, **2**, 674.

*Received March 16, 2015;*
*in revised form June 9, 2015*